

## Chapter 2

# Using Molecular Modeling Trending to Understand Dielectric Susceptibility in Dielectrics for Display Applications

Nancy Iwamoto, Ahila Krishnamoorthy and Edward W. Rutter Jr

This paper is based upon “Understanding Leakage Current Susceptibility in Dielectrics using Molecular Modeling”, which appeared in the Proceedings of Eurosime © 2009, IEEE.

**Abstract** Dielectric materials are universally used in the fabrication and packaging of microelectronic and display devices, as well as used in discrete devices such as sensors, switches and photovoltaics. However, as device and interconnect sizes become smaller, the question of the source of electrical failure becomes more and more important. During the development of these materials it has been found that small changes in the molecular structure can lead to small increases in conductivity which is undesirable for most applications. Although important to the final commercial acceptance of the dielectric, leakage current is often one of the final properties measured when developing the chemistry of the dielectric, so a dielectric with very good mechanical properties can ultimately fail at end-user applications due to the poor electrical properties. Knowledge of the susceptibility for electrical failure can be a great aid to the developer, and molecular modeling used in a trend analysis has been found useful to predict tendencies.

## 2.1 Introduction and Problem Focus

This paper focuses on the use of molecular modeling to help explain experimental observations during the development of thick film dielectrics for application in flat panel displays (FPD). The layer configurations used in these displays are

---

N. Iwamoto (✉) · A. Krishnamoorthy · E. W. Rutter Jr  
Honeywell Specialty Materials, 1349 Moffett Park Drive,  
Sunnyvale, CA 94089, USA  
e-mail: nancy.iwamoto@honeywell.com

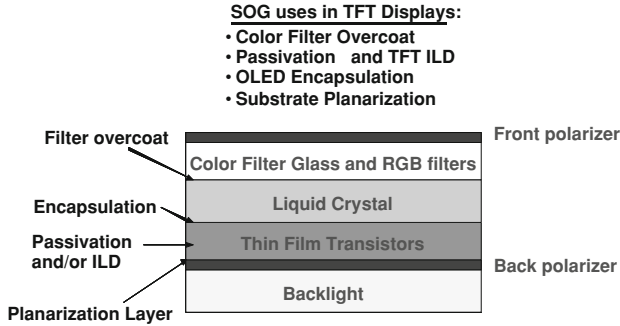


**Fig. 2.1** General layer build-up in a display

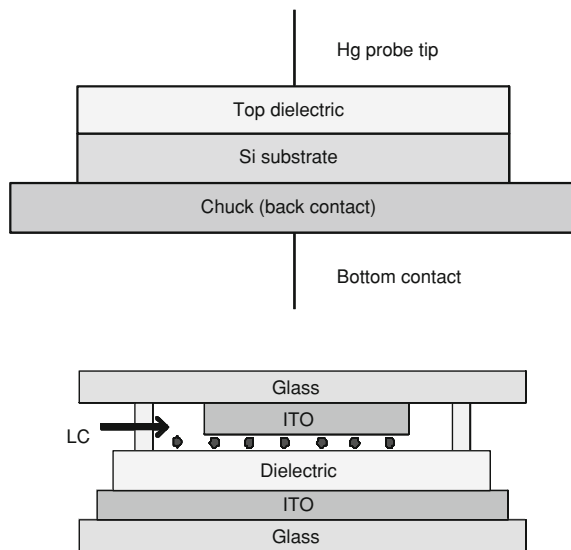
well-known [1] and a schematic is found in Fig. 2.1. The traditional spin-on-glass (SOG) formulation may have an application in many of the different layers used, including uses such as planarization, passivation and encapsulant layers, however the materials under development in the current work were used as encapsulant layers next to the liquid crystal layer.

As may be envisioned in such a multi-layer configuration, if materials are to be correctly integrated, the electrical effects on the total performance of the display should be understood. Since the target material application involved the encapsulation layer next to the liquid crystal, it was important to show that the dielectric under development would not interfere with the switching of the liquid crystal, and molecular modeling was found to be very useful in that understanding.

The electrical properties of the dielectric was characterized by measuring leakage current on a planar film and also by determining the ability to hold voltage in a liquid crystal test cell commonly known as voltage holding ratio or VHR tests. The test configurations are shown in Fig. 2.2. During actual material development, the easiest test to reproduce for the material developer is the leakage current test which employs a typical mercury probe in contact with the dielectric film formed on silicon wafer, creating capacitor. If the mercury-sample contact is ohmic (non-rectifying) then current–voltage instrumentation can be used to measure leakage currents, or current–voltage characteristics. The same mercury-sample structures can be measured with capacitance–voltage instrumentation to monitor permittivity (dielectric constant) and thickness of dielectric materials so the measurements are a convenient gauge for development of novel dielectrics. The VHR test is the most important test to evaluate the dielectric encapsulant. The test is done on a fabricated liquid crystal test cell with stacks of liquid crystal, dielectric and the metal to form contacts. A fixed bias is applied between two metal electrodes encompassing liquid crystal and dielectric and the voltage monitored with time. A good dielectric does not affect the voltage held, so that there is no degradation in the polarization (and therefore display image quality) of the liquid crystal.

Both tests suggest that either conductivity issues or dielectric constant issues are involved in signal loss, but the tests themselves do not help the material developer understand root issues of performance. Specifically for the performance

**Fig. 2.2** *Top* Test configuration for leakage current; *Bottom* Test cell for voltage holding ratio (VHR)



of the dielectric used next to the liquid crystal layer (LC), a distinct concern is identifying the major mechanism responsible for any signal loss in order to develop dielectrics that do not impact the performance of the display LC. So although tests are well-known, the ties to the material structures which would help guide material development are absent and molecular modeling was engaged to help fill the gaps in understanding.

Many examples exist in the literature using quantum mechanics for screening conducting materials [2, 3], but fewer references are associated with issues surrounding the electrical performance of dielectrics in applications. Molecular modeling is not usually used for investigating conduction problems in dielectrics. For leakage current it was decided that value might be placed on looking at relative band diagrams (relative conductivity potential) to look for trends in band gap and mobility. As will be discussed in this paper, it was found that exact band structures are not necessary to understand what is happening to the material, as long as adequate benchmarks of known materials have been calculated and comparisons are kept within groups. In this manner, the calculations of interest may be simple, without requiring large unit cells or high levels of theory and we have found that building simple band structure trends are useful in understanding the current leakage trends in our materials under development. For VHR, it was also found that molecule polarization was of great help to correlate the testing to that of the material, as it was decided that this quality best represented the molecular structural quality to respond to an external field.

In all cases, CASTEP, a plane-wave pseudo-potential code based on density functional theory (DFT) from Accelrys Inc. [4–9] has been used employing ultrasoft norm-conserving pseudo-potentials. The generalized gradient

approximation (GGA) exchange-correlation was used along with the PBE local density functional, Gaussian smearing and Pulay density-mixing. All calculations made use of periodic unit cells, in which the bonding was adjusted to maintain infinite bonding in at least two, if not all three dimensions.

It should be emphasized that since the modeling was not meant to determine exact values all comparisons made were for directional purposes only. Care has been taken to compare comparable structures to minimize variation in structure outside of the subject query. In addition because of the proprietary nature of all formulations specific structures concerning the dielectric materials under development cannot be reported.

## 2.2 Results

### 2.2.1 Model Benchmarks to Experiment

In order to identify trends in calculations, simple experimental cases were used to benchmark the leakage current trends by looking specifically for bandgap changes in the band structure. In addition, cases from the literature were used to benchmark calculated molecular polarizability (for VHR).

One well-known benchmark that was qualified was the effect of silanol content. It is known that the presence of SiOH (silanol) groups increase the leakage of silicate films; usually found when films are not cured or cross-linked completely as shown in Fig. 2.3. As shown in Table 2.1, the effect of low-temperature curing which enhances silanol content is to decrease the breakdown voltage (at 1  $\mu\text{A}$  and 1  $\mu\text{A}/\text{cm}^2$  in the last two columns) represented as field to breakdown (FBD) expressed in MV/cm and as a result the films have increased leakage current.

Example structures were built for band-structure calculations, which involved full silicate bonding and then bond cleaved to form partial silicate bonding, terminated in SiOH groups (Fig. 2.4). As expected, qualitatively there is a difference between the band structures, showing that when SiOH is present, the bandgap shrinks (as defined by the gap between the valence band at zero, and the conduction band, which is the next band above it) from around 6 eV to around 4 eV. As further indication that conditions encouraging leakage are being formed, the valence band curvature is increasing suggesting an increased hole mobility.

In addition, another comparison was made using well-known substitution effects observed in-house. Table 2.2 shows the test comparisons of two different functional groups that have been commonly used during dielectric development. Testing in our laboratories found that group R1 will consistently leak and R2 will not. Figure 2.5 shows the calculated bandstructures starting with the same structure using R1 (*left*), then substituting R2 (*right*) for R1. In this comparison, the bandgaps seem to be similar. Because of the size differences in the R1 and R2 groups, the bandgap comparison was further qualified by adjusting densities using

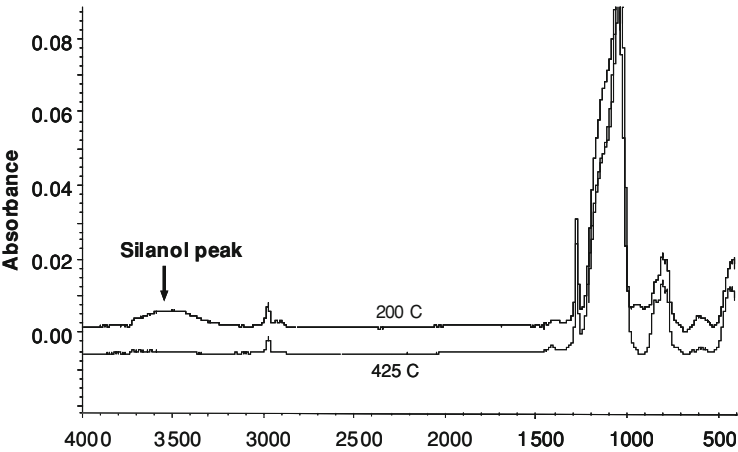


**Fig. 2.3** FTIR of differently cured SOG films showing the higher SiOH region for the lower-temperature cures

**Table 2.1** Effect of cure on field breakdown

#	Cure temp	Dielectric constant, k (Hg probe)	FBD measured at constant current 1 A (MV/cm)	FBD measured at constant current density 1 A/cm <sup>2</sup> (MV/cm)
1	250°C/60 min	3.44	3.28	3.04
2	250°C/60 min	3.43	3.34	3.08
3	425°C/60 min	3.11	3.78	3.57
4	425°C/60 min	3.11	3.64	3.51

different configurations (cage and opened-cage rings) so that the most stable unit cell (lowest energy) was obtained for both R1 and R2. When these band structures were compared, the conclusion was the same: the bandgaps are the same at around 4 eV. The biggest difference between the structures is that the curvature for the conduction band of R1 is highly accentuated suggesting a much higher electron mobility.

These two examples suggest that as we look at comparisons, both the band gaps and the mobility (as inferred by the curvature) should be monitored. Because mobility or effective mass became a metric to monitor, benchmarks for mobility was also estimated based upon curvature slope in the band structures (estimation technique was developed by Accelrys [3–9]). The benchmarks for the mobility trends are found in Table 2.3, showing that qualitatively the direction of mobility is the same as reported in the literature.

The effective masses for all structures obtained for comparing silanol effects, R1 and R2 were calculated and compared to look for general trends; these results are shown in Table 2.3 and Fig. 2.6. As a group, clearly the lowest effective

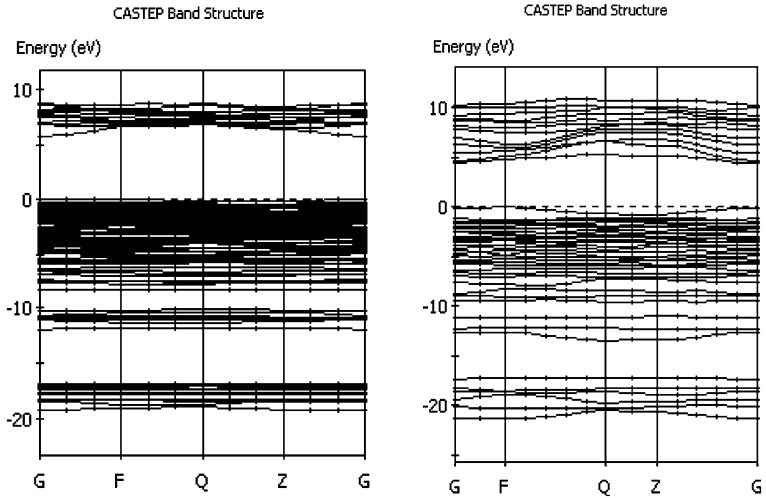


**Fig. 2.4** Band structure of a silicate before (*left*) and after (*right*) bond cleavage to form SiOH groups

**Table 2.2** Experimental tests of group R1 versus R2

#	Refractive index	Dielectric constant, k	FBD measured at constant current 1 $\mu$ A (MV/cm)	FBD measured at constant current density 1 $\mu$ A/cm <sup>2</sup> (MV/cm)
1	250°C/60 min	3.44	3.94	2.62
2	250°C/60 min	3.43	3.61	3.27
3	425°C/60 min	3.11	4.47	4.41
4	425°C/60 min	3.11	4.47	4.42

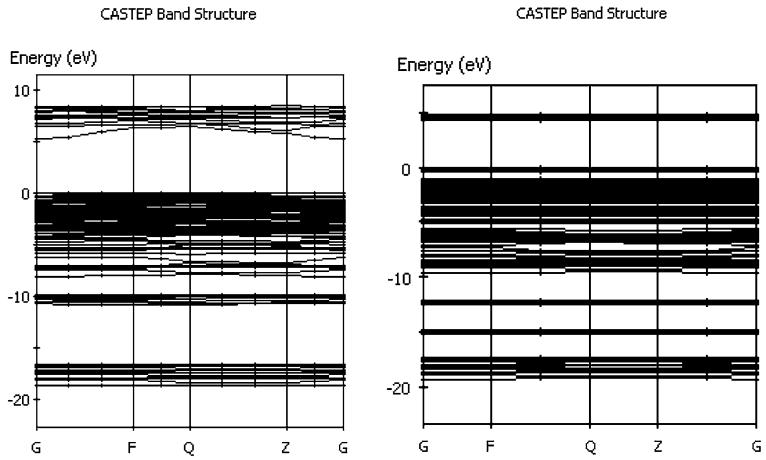


**Fig. 2.5** Band structures of silicates with R1 (*left*) versus R2 (*right*)

**Table 2.3** Effective mass estimates compared to the literature

	Literature [10, 11]		Calculated	
	Effective mass (me)		Effective mass (me)	
	Hole	Electron	Hole	Electron
Si	1.56 [10]	1.08 [10]	0.74	1.76
Ge	0.37 [10]	0.56 [10]	0.65	1.13
In <sub>2</sub> O <sub>3</sub>	0.6 [11]	0.3 [11]	0.72	0.22

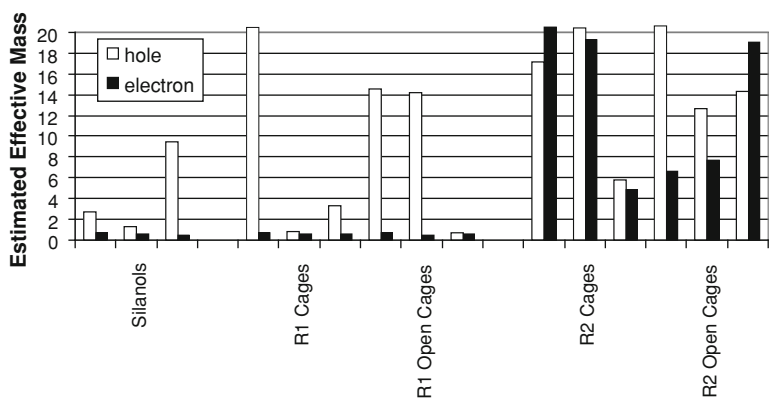


**Fig. 2.6** Effective masses compared across functional group types

**Table 2.4** Polarizability of PVDF

	CHEMOS: Hartree–Fock, CNDO [12]	CASTEP: DFT GGA/PBE	
	(Å <sup>3</sup> )	Optical (Å <sup>3</sup> )	Static (Å <sup>3</sup> )
PVDF (all trans)	~9.05	9.03	11.1
PVDF (cis/trans)	~8.8	8.07	10.3

masses and so the most conductive are those grouped with silanol content, followed by the R1 structures. The R2 structures, as a group definitely have the highest effective masses and so overall should have the least issues with leakage current.

As will be discussed later, polarizability calculations were found to be specifically important to understand VHR and the calculations were first benchmarked against the literature using a well-known piezoelectric polymer, polyvinylidene-fluoride (PVDF). As shown in Table 2.4, even though different methods are used from the literature, the current calculations adequately represent the decrease in polarizability as the cis isomer is introduced and there is high agreement in values for the trans isomeric form with exact matches in structure.

**Table 2.5** Leakage results for two different Formulations A and B

Formulation	Refractive index	Dielectric constant, k	FBD measured at constant current 1μA (MV/cm)	FBD measured at constant current density 1μA/cm <sup>2</sup> (MV/cm)
A	1.5002	3.48	4.58	2.09
A	1.5009	3.50	4.32	2.48
B	1.5115	3.83	3.69	1.76
B	1.5114	3.84	3.59	1.75

**2.2.2 Leakage Comparisons to Bandstructure**

The most important aspect of this work was to determine the electrical performance trends of actual formulations, and there were two major formulation types that were of concern. The leakage results are shown in Table 2.5, obviously showing that Formulation B has much lower breakdown voltage, and so should be highly leaky.

The band structures of these two formulations were obtained, using different densities to ensure that a good range of possibilities were considered. Because of a basic functional group difference in one of the components in Formulation B, densities were obtained assuming a low-cure (cure 1) and a high-cure (cure 2) situation with different extents of cross-linking. The results are compiled in Fig. 2.7. As a group, formulation B consistently has lower bandgap properties than formulation A. It appears that if formulation B attains a higher cure, and higher densities, the band gap may suddenly drop. The effective masses were determined and represented in Table 2.6. In general the effective masses are high for both formulations, except for one case in Formulation B where the effective masses are low enough to have serious concerns for leakage. As mentioned previously, leakage current experiments suggest that Formulation B is highly leaky. The decision based on this result would have been not to use this material in any device that needs this functional requirement.

To further test differences between the two formulations and to see whether there are any unexpected interface quality issues with the liquid crystal (LC) or polyimide (PI) interface that might be present in the actual display, the interaction energies of each formulation were calculated with test cases derived from the literature that might be representative of possible polymers (LC or PI) used in device fabrication to test whether there is a fundamental difference between interfaces made with Formulation A and B. Two test cases were used for each polymer shown in Fig. 2.8, where unit cells were built from a layer of the polymer and a layer of the formulation. The formation energies of this interface were compared to formation of a free surface (Fig. 2.10). In all cases, Formulation B appears to have a weaker interface. To further check on the electrical properties of the interface, the band gaps and effective masses of the interface unit cells were determined. These results are found in Table 2.7, showing that in general the band



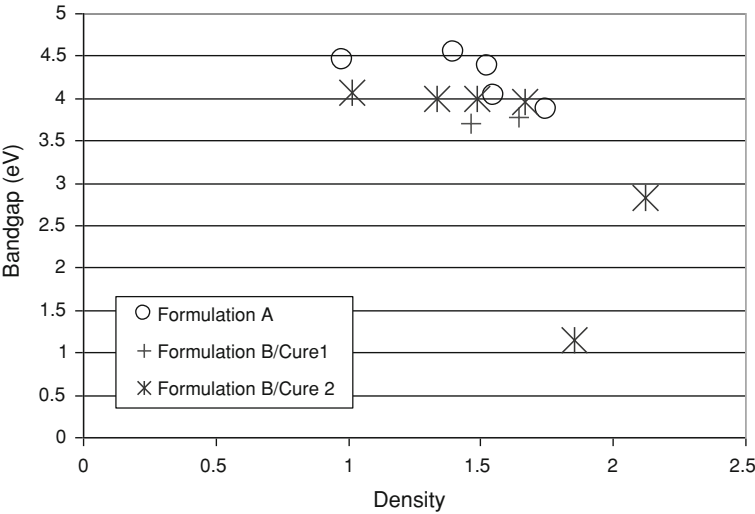


Fig. 2.7 Band gap (Fermi to conduction band gap in eV) comparisons of Formulations A and B

Table 2.6 Effective masses (mobility) for Formulations A and B

	Density	Bandgap (eV)	Hole effective mass	Electron effective mass
Formulation A	1.5	4.38	84.01	21.34
Formulation A	1.6	4.03	27.65	2.82
Formulation B/cure1	1.6	3.78	152.45	5.87
Formulation B/cure1	1.5	3.71	65.59	21.21
Formulation B/cure2	1.7	3.97	11.03	14.61
Formulation B/cure2	1.4	3.99	–	0.88

gaps are similar (it may be argued that Formulation B has a slightly lower band gap) and all interfaces have relatively high-effective masses, so do not have mobile carriers. That is, there is no reason to believe that the interface contributes to the leakage due to carriers.

2.2.3 VHR and Polarization Comparisons

The most important electrical test for acceptance of the dielectric encapsulant is the voltage holding ratio (VHR) test. As explained previously it requires the fabrication facility to prepare a test cell and is more time consuming. The results for formulation A and B are found in Fig. 2.9. These figures show that films from Formulation B are better at holding the voltage bias, which is surprising since Formulation B showed higher leakage tendencies.

**Fig. 2.8** **a** Two common LC structures used to test formulation interface stability. (*Top* is designated LC1, and *bottom* is designated LC3). **b** Two common polyimide structures used to test formulation interface stability (*Top* is designated PI1, and *bottom* is designated PI5)

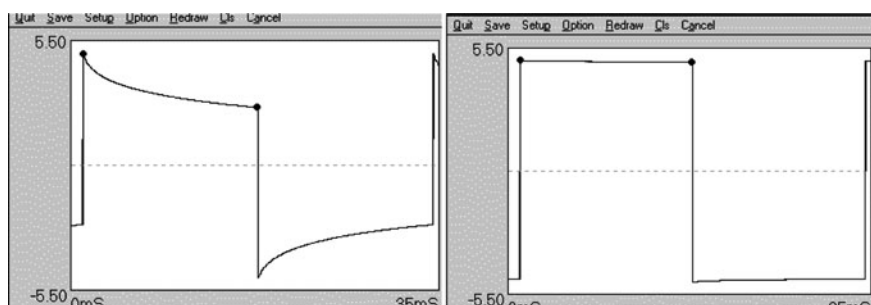
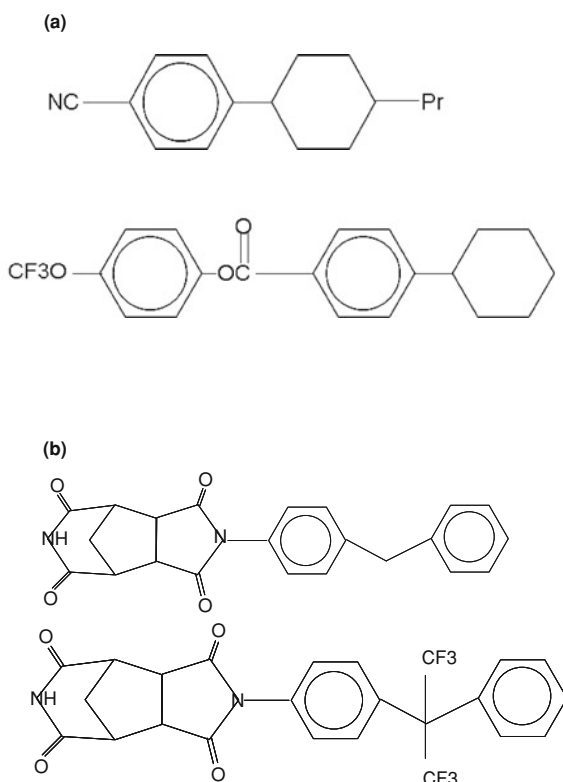


**Fig. 2.9** VHR test results. *Left*: Formulation A; *Right*: Formulation B

Since voltage holding is directly related to how well a dielectric may hold its charge, which is in turn related to how well a structure may hold polarization, the polarizabilities of the formulations were determined. Figure 2.10 shows the calculated polarizabilities of each formulation using several different densities; for Formulation B the high- and low-cure structures were also used. Consistent with

**Table 2.7** Relative effective masses of interface structures

Interface representation	Bandgap	Effective mass estimate (me)	
		Hole	Electron
Formulation A surface	4.38	39.25	54.64
Formulation A-LC1	3.95	6.69	19.38
Formulation A-LC3	3.47	87.60	237.12
Formulation A-PI1	3.31	317.72	10.74
Formulation A-PI5	3.6	41.19	70.71
Formulation B/cure2 surface	3.93	5.03	11.27
Formulation B/cure2-LC1	3.3	28.73	18.62
Formulation B/cure2-LC3	3.31	23.45	29.88
Formulation B/cure2-PI1	3.19	87.12	21.51
Formulation B/cure2-PI5	3.22	17.67	262.14

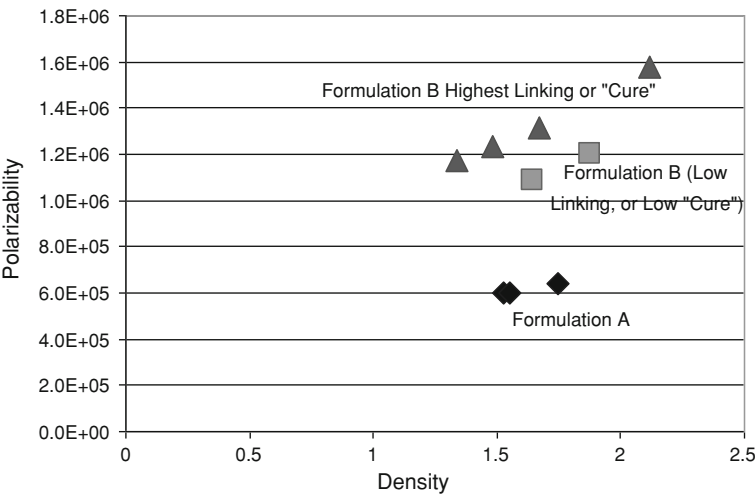


**Fig. 2.10** Polarizability of Formulations A and B (B is shown for two different cure states)

the stable VHR, Formulation B consistently has the higher polarizability. This trend also agrees with the higher measured dielectric constant of Formulation B than Formulation A (Fig. 2.10).

2.3 Discussion and Conclusions

When compared against the experimental results, the modeling results appear to be consistent within tests. That is, leakage trends are consistent with bandgap trends and estimated effective masses hint at which structures may be more susceptible to leakage; and the voltage holding ratio tests are consistent with the polarizabilities

of the structures, showing the importance of polarity within the structures adding to the overall capacitance.

However, the two results seem counter-intuitive to one another if it assumed that leakage is a major detractor to switching performance and display instability while high VHR indicates better performance. These results suggest that for these dielectrics the more important contribution comes from the native capability for polarization and so it performs as a better dielectric in contact with liquid crystal. In addition, charge carrying capability does not appear to be significant for the dielectric's role judging from similarly high-effective masses for both formulations. So, the higher polarizability of Formulation B and so its higher dielectric constant suggests that it should perform like a better dielectric and higher voltages should be sustained before carriers can be developed, dielectric breakdown occurs and conduction mechanisms are dominant. However the recent models and tests do not answer when such polarization/capacitance mechanisms give rise to internal carrier generation and leakage, or at what point this mechanistic change becomes important to the display performance. Interestingly, Formulation B also has less interface interaction between the LC and the dielectric. Looked at in another way, the dielectric might help LC phase transformation just because of lower friction/stiction. If this is the case there are clearly more mechanistic issues that could be addressed from the film interaction aspect [13, 14] including, the role of adhesion and wetting at the interface and what balance must exist at the layer interfaces for the dielectric to help LC performance without layer delamination.

Overall, the modeling shows that it can be used to help separate performance effects from the structural level, as well as help understand issues from the device side. For instance these calculations did help to highlight the polarization effects and show that these effects may be related to VHR, further separating the mechanism from those effects derived from conductivity to carrier generation. Interestingly the leakage tendencies do match bandgap and mobility trends, even though such calculations are reserved for more conductive materials, so as a qualitative tool for non-conductive materials, the calculation can still be used. Generally, we have found that such models used to gauge electrical effects do not have to be quantitatively perfect in order to aid the material developer, but care must be observed in comparisons (benchmarks used) so that the emerging trends may be trusted.

**Acknowledgments** The authors would like to acknowledge discussions held with Stephen Yates and Kenneth Heffner of Honeywell Aerospace that helped us justify looking into at band-structure trends for leakage susceptibility. Although all statements and information contained herein are believed to be accurate and reliable, they are presented without guarantee or warranty of any kind, express or implied. Information provided herein does not relieve the user from the responsibility of carrying out his own tests and experiments, and the user assumes all risks and liability for use of the information and results obtained. Statements or suggestions concerning the use of materials and processes are made without representation or warranty that any such use is free of patent infringement and are not recommendations to infringe any patent. The user should not assume that all toxicity data and safety measures are indicated herein or that other measures may not be required.

## References

1. Lee JH, David NL, Shin-Tson Wu (2008) Introduction to flat panel displays. Wiley, UK
2. Ren CY, Chiou SH, Choisset J (2006) First-principles calculations of the electronic band structure of  $\text{In}_4\text{Sn}_3\text{O}_{12}$  and  $\text{In}_5\text{SnSbO}_{12}$ . *J Appl Phys* 99:023706
3. Zgou H, Bouzzine SM, Bouzarkraoui S, Hamidi M, Bouacrine M (2009) Theoretical study of structural and electronic properties of oligo(thiophene-phenylene)s in comparison with oligothiophenes and oligophenylenes. *Chin Chem Lett* 19:123–126
4. Accelrys, Inc. San Diego, CA (CASTEP was employed under Materials Studio 4.3 for these calculations)
5. Segall MD, Lindan PJD, Probert MJ, Pickard CJ, Hasnip PJ, Clark SJ, Payne MC (2002) First-principles simulation: ideas, illustrations and the CASTEP code. *J Phys: Cond Matt* 14:2717–2744
6. Kohn W, Sham LJ (1965) Self-consistent equations including exchange and correlation effects. *Phys Rev* 140:A1133
7. Vanderbilt D (1990) Soft self-consistent pseudopotentials in a generalized eigenvalue formalism. *Phys Rev B* 41:7892–7895
8. Perdew JP, Burke K, Ernzerhof M (1996) Generalized gradient approximation made simple. *Phys Rev Lett* 77:3865–3868
9. Alibert C, Skouri M, Joullie A, Benouna B, Sadig S (1991) Refractive indices of AlSb and GaSb-lattice matched  $\text{Al}_x\text{Ga}_{1-x}\text{As}_y\text{Sb}_{1-y}$  in the transparent wavelength region. *J Appl Phys* 69:3208–3211
10. Sze Simon M, Kwok K Ng (2001) Physics of semiconductor devices. Wiley, Chichester
11. Zheng MJ, Zhang LD, Zhang XY, Zhang J, Li GH (2001) Fabrication and optical absorption of ordered nanowire arrays embedded in anodic alumina membranes. *Chem Phys Lett* 334:298–302
12. Correia Helena MG, Ramos Marta MD (2005) *Comput Mater Sci* 33:224–229
13. Iwamoto N, Krishnamoorthy A, Spear R (2009) Performance properties in thick film silicate dielectric layers using molecular modeling. *Microelectron Reliab* 249:877–882
14. Iwamoto N, Li T, Sepa J, Krishnamoorthy A (2007) Dielectric constant trends in silicate spin-on-glass. SPIE Nanoengineering: fabrication, properties, optics and devices IV session, conference 6645, San Diego, 26–30 August 2007

Molecular Modeling and Multiscaling Issues for  
Electronic Material Applications

Iwamoto, N.; Yuen, M.; Fan, H. (Eds.)

2012, XII, 260 p., Hardcover

ISBN: 978-1-4614-1727-9